BIOCHEMISTRY
including biophysical chemistry & molecular biology
Article

Biochemistry **2009,** *48,* 5631–5641 5631
DOI: 10.1021/bi9002138

Glycosylated SV2 and Gangliosides as Dual Receptors for Botulinum Neurotoxin Serotype F[†,‡]

Zhuji Fu,[§] Chen Chen,[∥] Joseph T. Barbieri,[∥] Jung-Ja P. Kim,[§] and Michael R. Baldwin*,[∥]

[§]*Department of Biochemistry, and* [∥]*Department of Microbiology and Molecular Genetics, Medical College of Wisconsin, 8701 Watertown Plank Road, Milwaukee, Wisconsin 53226*

Received February 9, 2009; Revised Manuscript Received May 14, 2009

ABSTRACT: Botulinum neurotoxin causes rapid flaccid paralysis through the inhibition of acetylcholine release at the neuromuscular junction. The seven BoNT serotypes (A−G) have been proposed to bind motor neurons via ganglioside−protein dual receptors. To date, the structure−function properties of BoNT/F host receptor interactions have not been resolved. Here, we report the crystal structures of the receptor binding domains (HCR) of BoNT/A and BoNT/F and the characterization of the dual receptors for BoNT/F. The overall polypeptide fold of HCR/A is essentially identical to the receptor binding domain of the BoNT/A holotoxin, and the structure of HCR/F is very similar to that of HCR/A, except for two regions implicated in neuronal binding. Solid phase array analysis identified two HCR/F binding glycans: ganglioside GD1a and oligosaccharides containing an *N*-acetyllactosamine core. Using affinity chromatography, HCR/F bound native synaptic vesicle glycoproteins as part of a protein complex. Deglycosylation of glycoproteins using α(1-3,4)-fucosidase, endo-β-galactosidase, and PNGase F disrupted the interaction with HCR/F, while the binding of HCR/B to its cognate receptor, synaptotagmin I, was unaffected. These data indicate that the HCR/F binds synaptic vesicle glycoproteins through the keratan sulfate moiety of SV2. The interaction of HCR/F with gangliosides was also investigated. HCR/F bound specifically to gangliosides that contain α2,3-linked sialic acid on the terminal galactose of a neutral saccharide core (binding order GT1b = GD1a ≫ GM3; no binding to GD1b and GM1a). Mutations within the putative ganglioside binding pocket of HCR/F decreased binding to gangliosides, synaptic vesicle protein complexes, and primary rat hippocampal neurons. Thus, BoNT/F neuronal discrimination involves the recognition of ganglioside and protein (glycosylated SV2) carbohydrate moieties, providing a structural basis for the high affinity and specificity of BoNT/F for neurons.

Botulinum neurotoxins (BoNTs) inhibit neurotransmitter release by cleaving one or more components of the vesicular fusion machinery. BoNTs are single chain AB toxins that comprise an N-terminal light chain protease (LC) that is disulfide linked to a C-terminal heavy chain that includes a translocation domain (HCT) and a receptor binding domain (HCR). BoNTs are divided into seven serotypes (termed A−G) based on the lack of antitoxin cross-neutralization. While experimental evidence suggests that humans are sensitive to all serotypes, natural intoxications are associated with serotypes A, B, E, and F (*1*−*4*). In addition, BoNT/A[1], BoNT/B, and BoNT/F have also been used as therapeutic agents for the treatment of neurological disorders in humans (*1*, *3*).

The prototype strain of *Clostridium botulinum* type F was first isolated as a source of human botulism on the Danish Island, Langeland (*5*). BoNT/F Langeland is a 1274-amino acid protein possessing a toxic potency similar to other BoNT serotypes (*6*). Subsequent studies demonstrated that strains of *C. barati* isolated from cases of infant botulism also produced a BoNT/F neurotoxin (*7*−*10*). The delayed recognition of BoNT/F as a toxin of humans was probably linked to misidentification of type F, due to cross-neutralization by type E antitoxin (*9*). The molecular basis for cross-neutralization is not currently understood, but is suggested to be linked to the high sequence homology between

[†]This work was supported by grants from the Great Lakes Regional Center of Excellence (GLRCE) from NIH-NIAID U54 AI057153 (to J.T.B. and J.-J.K.) and NIH-NINDS K99 NS061763 (to M.R.B.). Results shown in this article are derived from work performed at Argonne National Laboratory, Structural Biology Center at the Advanced Photon Source. Argonne is operated by UChicago Argonne, LLC, for the U.S. Department of Energy, Office of Biological and Environmental Research under contract DE-AC02-06CH11357.

[‡]The atomic coordinates and structure factors (pdb code 3FUO for HCR/A and 3FUQ for HCR/F) have been deposited in the Protein Data Bank, Research Collaboratory for Structural Bioinformatics, Rutgers University, New Brunswick, NJ.

*To whom correspondence should be addressed. Tel: 414-456-8419. Fax: 414-456-6535. E-mail: mbaldwin@mcw.edu.

[1]Abbreviations: BoNT/A, botulinum neurotoxin serotype A; BoNT/F, botulinum neurotoxin serotype F; HCR/F, heavy chain receptor binding domain of BoNT serotype F; HCR/A, heavy chain receptor binding domain of BoNT serotype A; HCR/T, heavy chain receptor binding domain of Tetanus neurotoxin; VAMP2, vesicle-associated membrane protein 2; SNAP25, synaptosomal-associated protein of 25 kDa; SNARE, soluble NSF attachment receptor; DIV, days *in vitro*; KS, keratan sulfate.

Published on Web 05/19/2009

BoNT/E and BoNT/F (*11*). To further understand the mechanisms of cross-neutralization, a detailed structure−function analysis of BoNT/F is required.

BoNTs target the presynaptic membranes of α-motor neurons through molecular mechanisms that are only now being defined. A dual receptor model for BoNT intoxication was proposed by Montecucco and co-workers (*12*) where BoNTs initially interact with glycolipids such as gangliosides, concentrating the toxin on the presynaptic membrane. Subsequent to initial capture, BoNTs interact with a second glycolipid and/or protein coreceptor triggering receptor-mediated endocytosis. Recent studies employing structural, biochemical, and genetic approaches have supported this model for BoNT serotypes B and G (*13*−*17*).

Gangliosides are complex lipids with a strong amphiphilic character due to the large oligosaccharide headgroup and the double-tailed hydrophobic moiety. The lipid moiety of gangliosides is constituted by the long-chain alcohol sphingosine, connected to a fatty acid by an amide linkage. The oligosaccharide chain of gangliosides is variable because of the sugar structure, content, sequence, and linkages. Sialic acid is the sugar that differentiates gangliosides from neutral glycosphingolipids and sulfatides (*18*−*20*). Numerous reports have demonstrated that BoNTs bind directly to complex gangliosides (*15*, *21*−*27*) and that prior incubation of BoNTs with excess b-series gangliosides (GD2, GD1b, GT1b, and GQ1b) reduced toxicity both *in vitro* and *in vivo* (*22*). Mice unable to express complex gangliosides display lower sensitivity to BoNT/A, /B, /C, /E, and /G, while binding and entry of BoNT/A, /B, /E, and /G into cultured neurons lacking gangliosides is also diminished (*15*, *22*, *28*). Similarly, BoNT/F has been reported to bind GD1a, GD1b, and GT1b under conditions of low ionic strength, but a physiologic role for gangliosides has not been demonstrated (*24*).

In addition to ganglioside, recent studies have identified protein coreceptors for BoNTs, most completely defined for BoNT/B. Initial studies by Nishiki and co-workers showed that BoNT/B bound synaptotagmin II (*23*, *29*−*31*). Observing that the entry process of BoNT/B involved synaptic vesicle exocytosis, Chapman and colleagues proposed that synaptic vesicle proteins functioned as the physiological receptor for BoNT/B (*13*−*15*). Using luminal domain fragments of synaptic vesicle proteins fused to GST, synaptotagmin I (Syt I) and synaptotagmin II (Syt II) were shown to mediate the binding and entry of BoNT/B into cultured neuroendocrine cells and hippocampal neurons (*13*). Similar approaches demonstrated that Syt I and Syt II also mediate the binding and entry of BoNT/G (*17*), whereas SV2 mediates the binding and entry of BoNT/A and BoNT/E into cultured neurons (*28*, *32*, *33*). At present, the identity of the BoNT/F protein coreceptor remains unknown.

In the present study, the crystal structure of the receptor binding domain (HCR) of BoNT type F is reported. Structure-based functional studies characterized the molecular properties of the BoNT/F dual receptors, synaptic vesicle glycoprotein SV2, and gangliosides, both of which contribute to the high affinity interaction of BoNT/F with neurons.

EXPERIMENTAL PROCEDURES

Materials. Unless otherwise stated, molecular biology grade chemicals and reagents were obtained from Sigma-Aldrich Co. (St. Louis, MO). Restriction enzymes were from New England Biolabs. Neuronal cell culture reagents were from Invitrogen (Carlsbad, CA). Sprague−Dawley rat embryonic day 18 hippocampal neurons were from Brainbits LLC (Springfield, IL) and cultured as described by the supplier. The monoclonal antibody against VAMP-2 was obtained from Synaptic Systems (Germany). The monoclonal antibody α-SNAP-25-C (MC-6053, specific for cleaved SNAP25) was from R and D Antibodies (USA). The SV2 monoclonal antibody developed by Kathleen M. Buckley was obtained from the Developmental Studies Hybridoma Bank developed under the auspices of the NICHD and maintained by The University of Iowa, Department of Biological Sciences. *E. coli* codon optimized DNA constructs encoding HCR/A (Hall-A strain) and HCR/F (Langeland strain) were synthesized by EZBiolab (Westfield, IN). EIA 96-well flat bottom plates (Corning Costar plate 9018) were obtained from Thermo Fisher Scientific. Purified botulinum neurotoxin types A and F were provided by Dr. Eric Johnson, University of Wisconsin—Madison at levels below the limit exempted by the Centers for Disease Control and Prevention.

HCR Expression and Purification. DNA encoding HCR/A (residues 870−1295; Supporting Information, Figure 1) and HCR/F (residues 862−1278; Supporting Information, Figure 2) were subcloned into the pET-28 expression vector (Merck KGaA, Darmstadt, Germany). Mutated forms of HCR/F were generated using the Quikchange site-directed mutagenesis kit in accordance with the manufacturer's instructions (Stratagene). Purification of HCR/A and HCR/F from *E. coli* BL-21(DE3) was as described previously except that peak fractions from the S200-HR column were passed through a DEAE-sephacryl column prior to concentration with a second passage over Ni^{2+}-nitrilotriacetic acid resin (*34*). A typical purification from a 1-L culture yielded between 5 and 10 mg HCR/F and 15−25 mg HCR/A. The structural integrity of the mutated forms of HCR/F was estimated by performing limited proteolysis experiments measuring trypsin sensitivity.

Neutralization of BoNT Activity in Rat Hippocampal Neurons. Rat hippocampal neurons were cultured on poly-D-lysine coated glass coverslips in Neurobasal medium supplemented with 2 mM glutamine and B27 supplement for 10−14 days prior to use. Cells were treated with control solution (15 mM Hepes, 145 mM NaCl, 5.6 mM KCl, 2.2 mM $CaCl_2$, 0.5 mM $MgCl_2$, 5.6 mM glucose, 0.5 mM ascorbic acid, and 0.1% BSA at pH 7.4) or high K^+ solution (the same as the control solution but adjusted to 95 mM NaCl and 56 mM KCl) for 10 min at 37 °C, in the presence of 10 nM BoNTs with or without 1 μM of the indicated HCR. Cells were then washed with PBS and incubated for an additional 48 h at 37 °C in fresh Neurobasal medium/conditioned Neurobasal media (1:1). Following treatment, cells were washed three times with PBS, fixed with 4% w/v paraformaldehyde in PBS (15 min at RT), permeabilized with 0.1% Triton X-100/4% formaldehyde in PBS (for 10 min at RT), and stained with either mouse α-SNAP25-C or α-VAMP-2. Bound antibodies were visualized using α-mouse IgG Alexa488 (Invitrogen). Images were captured at room temperature using a Nikon TE2000 microscope equipped with a CFI Plan Apo VC 60X Oil, N.A. 1.4 type lens and a Photometrics CoolSnap ES camera. Image acquisition and subsequent analysis were performed using Metamorph version 7. Figures were compiled using Photoshop CS3 (Adobe).

Synaptic Vesicle Isolation and FLAG Immunoprecipitation. The isolation of partially purified synaptic vesicles (SG-V) from rat cerebral cortex was performed as described previously (*35*). The SG-V pool (~20 mL) was then layered on to a 900 mL column of Sephacryl-500HR equilibrated with buffered glycine (300 mM glycine, Hepes-OH at pH 7.4, and 0.1% w/v

sodium azide), overlaid with buffered glycine, and chromatography performed in buffered glycine at a flow rate of 60 mL/h, collecting 10-mL fractions. Western blotting of column fractions for the synaptic vesicle protein synaptophysin showed that synaptic vesicles were enriched approximately ~12-fold relative to initial synaptosomes. In contrast, the plasma membrane resident Na, K, ATPase (α-subunit) was not enriched in the SG-V fraction relative to the initial input and not detected in the final vesicle pellet. Final standardization of vesicle preparations was made by determining total protein content.

Detergent solubilization of synaptic vesicles and subsequent immunoprecipitation of 3×FLAG tagged HCR domains from vesicle lysates were performed as described previously (*36*).

Deglycosylation of Native Synaptic Vesicle Proteins. Triton X-100 soluble extracts of isolated synaptic vesicles (~250 μg total protein) were incubated alone or with 0.1 units each of α(1-3,4)- fucosidase, protein *N*-glycosidase F (PNGase F), and endo-β-galactosidase for 16 h at 37 °C. Treated samples were clarified by centrifugation (70,000*g*, 30 min) and then cooled to 4 °C prior to FLAG immunoprecipitation as described above.

The efficiency of oligosaccharide release was estimated using *Sambucus nigra* lectin (binding sialic acid) conjugated to HRP as follows. Triton X-100 soluble extracts (400 ng total protein per well) were applied to a high-protein binding 96-well plate in sodium carbonate buffer (pH 9.6) overnight at 4 °C. The plates were washed ×3 with PBS, and nonspecific binding sites were blocked by incubating for 1 h in sodium carbonate buffer (pH 9.6) with 2% w/v BSA. Binding assays were performed in 100 μL of PBS-1% w/v BSA/well for 2 h at 4 °C containing either purified HRP or at the indicated concentrations. Following incubation, plates were washed ×4 with PBS and bound lectins detected using TMB-Ultra (Pierce Biochemicals) as the substrate for HRP. The reaction was terminated by the addition of 0.2 M H_2SO_4, and the absorbance at 450 nm was determined using a plate reader (Victor 3 V, Perkin-Elmer) (Supporting Information, Figure 3). Under the conditions described above, increased release of oligosaccharides was not observed with a further addition of enzymes or extending the incubation time.

Ganglioside Binding Assay. Purified bovine brain gangliosides (Matreya, LLC) dissolved in dimethyl sulfoxide (20 mg/mL) and diluted in methanol were applied to nonprotein binding 96-well plates (1 or 10 μg gangliosides/well as indicated). The solvent was evaporated at RT, and the wells were washed ×3 with PBS. Nonspecific binding sites were blocked by incubating for 1 h in sodium carbonate buffer (pH 9.6) with 2% w/v BSA. Binding assays were performed in 100 μL of PBS/well for 2 h at 4 °C containing either HCR/A or HCR/F at the indicated concentrations and an α-FLAG M2 monoclonal antibody-HRP conjugate (diluted 1/10000, Sigma-Aldrich). Following incubation, plates were washed ×4 with PBS and bound HCR detected using TMB-Ultra (Pierce Biochemicals) as the substrate for HRP. The reaction was terminated by the addition of 0.2 M H_2SO_4, and the absorbance at 450 nm was determined using a plate reader (Victor 3 V, Perkin-Elmer).

Synaptic Vesicle Binding Assay. Crude synaptic vesicle membranes (LP2 fraction, 400 ng total protein per well) were applied to a high-protein binding 96-well plate in sodium carbonate buffer (pH 9.6) overnight at 4 °C. The plates were washed ×3 with PBS, and nonspecific binding sites were blocked by incubating for 1 h in sodium carbonate buffer (pH 9.6) with 2% w/v BSA. Binding assays were performed in 100 μL of PBS-1% w/v BSA/well for 2 h at 4 °C containing either wild-type HCR/F or the HCR/F^{W1250L} mutated protein at the indicated concentrations and an α-FLAG M2 monoclonal antibody-HRP conjugate (diluted 1/10000, Sigma-Aldrich). Following incubation, plates were washed ×4 with PBS, and bound HCR was detected using TMB-Ultra (Pierce Biochemicals) as the substrate for HRP. The reaction was terminated by the addition of 0.2 M H_2SO_4 and the absorbance at 450 nm was determined using a plate reader (Victor 3 V, Perkin-Elmer).

Protein−Glycan Interaction Screen. HCR/F was labeled with an Alexa Fluor 488 succinimidyl ester as described in the manufacturer's protocol (Invitrogen). Following extensive dialysis against Dulbecco's PBS to remove unincorporated dye, the molar HCR/dye ratio was determined (~1:1). The labeled HCR/F domain was screened by core H of the Consortium for Functional Glycomics (CFG) using array version 3.0. Protein (~200 μg/mL) was bound to the matrix in 20 mM Tris-HCL at pH 7.4, 150 mM NaCl, 2 mM $CaCl_2$, 2 mM $MgCl_2$, 0.05% Tween 20, and 1% bovine serum albumin (BSA) and quantified as described previously (*37*). The final data set is presented in Supporting Information, Figure 4.

Crystallization and Data Collection. Purified HCR/A or HCR/F was dialyzed and concentrated to 5−12 mg/mL in 30 mM Tris-HCl at pH 7.6 and 0.5 M NaCl. The hanging drops containing 2 μL of 12 mg/mL of HCR/A or 5 mg/mL of HCR/F protein and 2 μL of well solution were equilibrated against 0.5 mL well solution. For HCR/A, the well solution contained 0.1 M Hepes (pH 7.5), 12% polyethylene glycol 8000, 8% glycerol, and 100 mM NaCl, while the well solution for HCR/F contained 100 mM Tris-HCl (pH 8.5), 18% ethanol, and 150 mM NaCl. HCR/A was crystallized in the orthorhombic space group, $P2_12_12_1$ with cell dimensions a = 39.8 Å, b = 104.8 Å, and c = 112.8 Å. The HCR/F crystals belong to the monoclinic space group $P2_1$ with unit cell parameters of a = 42.3 Å, b = 74.1 Å, c = 74.8 Å, and β = 106.4°. There is one monomer in an asymmetric unit for both crystal forms. Diffraction data for HCR/A was collected at 100 K at the SBC 19ID beamline, Advanced Photon Source, Argonne National Laboratory, and data for HCR/F were collected using an R-AXIS IV^{+2} with a MicroMax 007 generator at 100 K. HKL2000 (*38*) was used for data processing. Data collection and processing statistics for both HCR/A and HCR/F crystals are summarized in Table 1.

Structure Determination and Refinement. Structures of HCR/A and HCR/F were solved by the molecular replacement method using MOLREP within the CCP4 program suite and using the structure of the HCR domain of the holotoxin A (residues 870−1295, pdb code, 3BTA) (*39*) as the probe for the HCR/A solution and the refined HCR/A structure as the probe for HCR/F structure determination. Initial structures from the molecular replacement results were refined using the program CNS (*40*). The refinement procedure consisted of rigid body and positional refinement followed by a simulated-annealing protocol. Iterative rounds of positional and temperature factor refinement followed by manual fitting and rebuilding using the graphics program TURBO-FRODO (*41*) with $2F_o - F_c$ and $F_o - F_c$ difference Fourier maps. At later stages of refinement, water molecules were assigned where electron densities were greater than 3 σ in the $F_o - F_c$ map and situated within 3.3 Å of a potential hydrogen bonding partner. The final models were completed with $R_{crystal}/R_{free}$ of 0.225/0.259 for HCR/A and 0.205/0.256 for HCR/F. A stereo image of HCR/A superimposed with HCR/F is shown in Figure 3. With the exception of the N-terminal 35 residues (6×His, 3×FLAG, and five N-terminal

Table 1: Data Collection and Refinement Statistics

protein	HCR/A	HCR/F
detector	Q315, SBC, APS	R-AXIS IV^{+2}
resolution/highest resolution shell (Å)	30−1.80 /1.86−1.80	30−2.05/2.12−2.10
total collected refs	282432	156554
unique refs	42220/4187	23953/1490
completeness (%)	94.6/96.1	91.8/58.0
redundancy	6.7/5.8	6.5/5.9
$\langle I/\sigma(I)\rangle$	32.6/17.1	44.8/13.6
space group	$P2_12_12_1$	$P2_1$
unit cell		
a, *b*, *c* (Å)	39.8, 105.1, 112.2	42.3, 74.2, 74.8
α, *β*, *γ* (°)	90, 90, 90	90, 106.4, 90
R_{sym}	0.069/0.564	0.037/0.125
Vm (Å^3/Da)/solvent content	2.3/45.6%	2.3/42.9%
mol. in ASU	1	1
no. of protein atoms	3423	3284
no. of water mol.	208	276
average *B* values (Å^2)		
protein main chain/ side chain atoms	20.9/23.0	19.8/21.2
water mol.	29.7	26.2
$R_{crystal}$	0.219/0.286	0.206/0.214
R_{free}	0247/0.337	0.243/0.265
rmsd from ideality		
bond length (Å)	0.006	0.006
bond angle (deg)	1.4	1.4

residues), the overall polypeptide fold of HCR/A (E875-L1295) is well-defined and essentially identical to those observed in the BoNT/A holotoxin structure (*39*).

RESULTS AND DISCUSSION

HCR/F Competes with BoNT/F Holotoxin for Binding to Primary Hippocampal Neurons. While Botulinum neurotoxin type F (BoNT/F) intoxicates the mammalian neuromuscular junction, the cellular determinants of host cell binding and internalization have not been resolved. A recombinant receptor binding domain (HCR/F) containing an N-terminal 3×FLAG epitope was engineered to analyze BoNT/F interactions with neuronal receptors. The ability of HCR/F to inhibit the intracellular activity of native BoNT/F holotoxin in rat hippocampal neurons was tested to validate this model system. Incubation of rat hippocampal neurons (DIV 10−14) with HCR/F resulted in dose-dependent association of the HCR, with binding properties similar to those of the HCR domain of serotype A (HCR/A) (Figure 1A). As reported previously, cleavage of SNAP25 by BoNT/A was enhanced by active synaptic vesicle recycling and was inhibited with a 100-fold molar excess of HCR/A (Figure 1B) (*13*, *32*, *36*). Cleavage of VAMP-2 by BoNT/F (*42*) was also enhanced by active synaptic vesicle recycling, implicating a role for synaptic vesicle protein(s) in the binding and entry of BoNT/F into neurons. Exposure of neurons to 100-fold molar excess HCR/F, but not HCR/A, reduced BoNT/F cleavage of VAMP-2 several-fold (Figure 1B). These data suggest that BoNT/F utilizes a unique receptor for neuronal intoxication relative to BoNT/A and that HCR/F binds to the physiological receptor of BoNT/F, which makes HCR/F a useful tool to characterize BoNT/F-host−receptor interactions.

HCR/F Binding to a Glycan Array. To gain insight into the mechanism of neuronal entry, the binding of HCR/F to a glycan array was determined. HCR/F labeled with Alexa-Fluor 488 (HCR/F-488) bound maximally to ganglioside GD_{1a} but did not

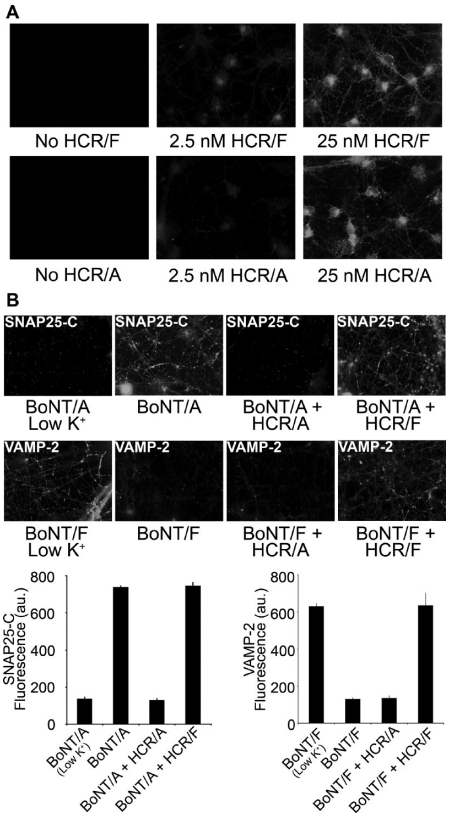

FIGURE 1: BoNT HCR domains inhibit the binding and entry of BoNT holotoxins into primary hippocampal neurons. (A) Hippocampal neurons (DIV 14) were exposed to HCR/A or HCR/F at the indicated concentrations for 30 min at 37 °C in HBSS. Cells were subsequently fixed, and bound HCRs were detected using an antibody against the 3× FLAG epitope. (B) Hippocampal neurons (DIV 10−14) were exposed to 10 nM BoNT/A or BoNT/F in the presence or absence of 1 μM HCR/A or HCR/F for 10 min at 37 °C. Cells were then rinsed and incubated for a further 48 h at 37 °C. Cleavage of SNAP25 by BoNT/A was detected using α-SNAP25-C that recognizes only the cleaved form of SNAP-25. SNAP25 cleavage by BoNT/A was reduced ∼85% by HCR/A ($P < 0.001$, *t*-test, $n = 32$), but not by HCR/F ($P > 0.05$, *t*-test, $n = 12$). Intact VAMP-2 was detected using an α-VAMP-2 antibody (clone 69.1), which detects only full length VAMP-2. VAMP-2 cleavage by BoNT/F was reduced ∼80% by HCR/F ($P < 0.001$, *t*-test, $n = 52$), but not by HCR/A ($P > 0.05$, *t*-test, $n = 38$). Error bars represent SEM.

interact with other ganglioside sugar moieties present on the array (Table 2 and Supporting Information, Figure 4). Of note, the glycan array did not include the ganglioside sugar moiety of GT_{1b} or GD_{1b}. In addition, HCR/F bound several glycan structures that contained *N*-acetyllactosamine [→Gal*β*(1 → 4) GlcNAc*β*(1→)] and 6O-sulfated derivatives, which forms the core repeating unit of keratan sulfate (Table 2). This observation suggested that HCR/F possessed two unique sugar binding domains.

Binding of HCR/F to Gangliosides Requires α2,3-Linked Sialic Acid on the Terminal Galactose of a Neutral Saccharide Core. There are reported quantitative and qualitative differences in the composition of gangliosides within the nervous system (*43*), which may contribute to the specificity of BoNT entry into neurons. Experiments were performed to extend the glycan array analysis to determine how HCR/F recognized gangliosides (Figure 2A, gangliosides tested GM_3, GM_{1a}, GD_{1a}, GD_{1b}, and GT_{1b}). While HCR/F bound to GT_{1b}, GD_{1a}, and GM_3 (potency of binding: $GT_{1b} = GD_{1a} \gg GM_3$), binding to GD_{1b} or GM_{1a} was not observed (Figure 2B). Increasing both the

Table 2: Glycan Array Analysis of HCR/F

glycan number	glycan	mean RFU[a]	% CV[b]
212[c]	NeuAcα2-3(NeuAcα2-3Galβ1-3GalNAcβ1-4)Galβ1-4Glcβ-Sp0 (**GD1a analogue**)	**39703**	**2**
220	Neu5Acα2-3Galβ1-3[6OSO3]GalNAcα-Sp8	21796	19
110	Galα1-4Galβ1-4GlcNAcβ-Sp8	17163	15
248	Neu5Acα2-6Galβ1-4GlcNAcβ1-3Galβ1-4GlcNAcβ-Sp0	13150	28
32	[3OSO3]Galβ1-3GalNAcα-Sp8	12045	17
36	[3OSO3]Galβ1-4GlcNAcβ-Sp0	11854	17
13	α-L-Rhα-Sp8	11586	44
310	Manα1-3(Manα1-6)Manβ1-4GlcNAcβ1-4GlcNAcβ-Sp12	11518	15
84	GalNAcα1-3(Fucα1-2)Galβ-Sp8	9812	65
151	Galβ1-4GlcNAcβ1-6GalNAcα-Sp8	9661	61
202	Neu5Acα2-3Galβ1-3GalNAcα-Sp8	9466	21
226	Neu5Acα2-3Galβ1-3GlcNAcβ-Sp8	9328	14
35	[3OSO3]Galβ1-4[6OSO3]GlcNAcβ-Sp8	9119	61
236	Neu5Acα2-3Galβ1-4GlcNAcβ-Sp0	8968	38
113	Galα1-6Glcβ-Sp8	8790	58
275	Galβ1-3-(Galβ1-4GlcNacβ1-6)GalNAc-Sp14	7974	56
90	GalNAcβ1-3Galα1-4Galβ1-4GlcNAcβ-Sp0	7764	67
213	Neu5Acα2-3(Neu5Acα2-6)GalNAcα-Sp8	7713	36
11	α-L-Fuc-Sp8	7551	83
85	GalNAcα1-3GalNAcβ-Sp8	7476	49

[a] Relative fluorescence units. [b] Coefficient of variation. [c] GD1a sugar analogue of a ganglioside.

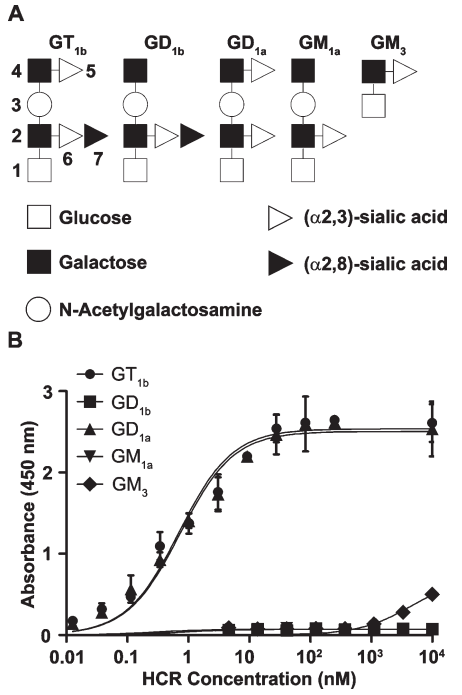

FIGURE 2: Binding of HCR/F to a panel of gangliosides. (A) Schematic of gangliosides used in this study (GT_{1b}, GD_{1b}, GD_{1a}, GM_{1a}, GM_3). Numbering of residues is based on standard nomenclature. (B) Gangliosides (10 μg per well) were coated onto nonbinding microtiter plates. HCR/F at the indicated concentrations was added to the plates in Dulbecco's PBS at 4 °C for 2 h in the presence of a HRP-conjugated anti-3×FLAG antibody. Plates were washed and bound HCR detected using ultra-TMB as a substrate for HRP. The data are the average of 3 independent experiments performed in quadruplet. The lines for ganglioside GT_{1b} and GD_{1a} lie on top of each other.

amount of immobilized GD_{1b} or GM_{1a} to 20 μg per well and HCR/F to 10 μM did not result in detectable binding (data not shown). Under identical conditions, saturable binding of tetanus HCR was detected indicating the presence of immobilized ganglioside (data not shown). These observations demonstrate that BoNT/F binds to gangliosides through interactions with an α2,3-linked sialic acid on terminal galactose residues and that the α2,8-linked sialic acid of GT_{1b} (denoted sia-7, Figure 2A) is not involved in ganglioside binding. The different ganglioside binding profile of HCR/F relative to HCR/T suggests that individual BoNTs utilize unique ganglioside recognition strategies.

Structure of HCR/F. The different ganglioside binding profile of HCR/F relative to HCR/T suggests these toxins may utilize unique ganglioside recognition strategies. To begin to address these potential differences, the crystal structure of HCR/F was determined. The structure of recombinant HCR/F was solved to 2.1 Å resolution by the molecular replacement method using the HCR/A structure (residues 875−1295) as the search probe. The entire HCR/F chain was visible except that the 1155−1160 and 1204−1209 loop regions and the N-terminal 36 residues (30 tagged residues plus residues 862−867) were disordered (Figure 3). The HCR/F molecule, 411 residues from D868 to N1278, had maximum dimensions of approximately 72 × 46 × 42 $Å^3$ and was composed of two subdomains of approximately equal size. The N-terminal domain (HCR_N, residues 868−1073) was formed from two antiparallel β-sheets connected such that the HCR_N domain was similar to the jelly roll domain found in many proteins. The C-terminal domain (HCR_C, residues 1085−1278) was linked to HCR_N through a single α-helix formed by residues (1074−1084) and adopted a modified β-trefoil fold (Figure 3).

The overall structure of HCR/F was similar to those of the HCR domain of native BoNT/A (pdb code: 3BTA (*39*)), recombinant HCR/A (Figure 3, this study), HCR/B (pdb code: 2NM1 (*16*)), and tetanus HCR (HCR/T, pdb code: 1YYN (*44*)). The root-mean-square (r.m.s.) deviation between HCR/F and HCR/A was 1.0 Å for 377 Cα atoms, 1.2 Å for 291 HCR/B Cα atoms, and 1.4 Å for 272 HCR/T Cα atoms. Thus, while the overall sequence homology is relatively low among BoNT/A, /B, and /F and TeNT, the respective HCR domains show structural similarity (*45*). The major differences between the

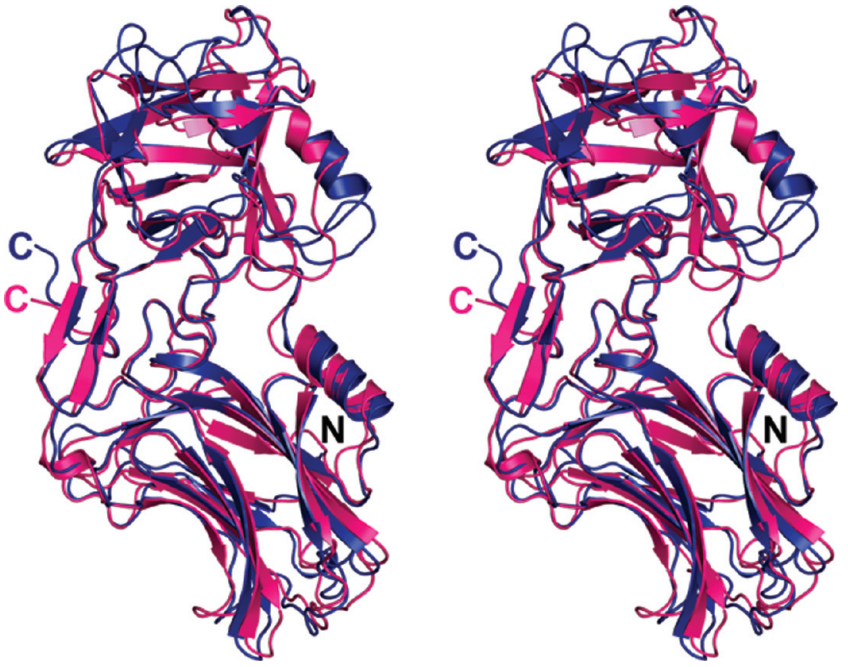

FIGURE 3: Stereo diagram of superposition of the structures of HCR/A (blue) and HCR/F (pink). N- and C-termini are labeled (N-terminus of both structures overlap, while the C-terminus in each structure is marked separately, dark blue for HCR/A and pink for HCR/F). The proteins are made of two distinctive domains, the N-terminal jelly roll domain (bottom) and the C-terminal β-trefoil domain (top). The overall structures of HCR/A and HCR/F are very similar with an rms deviation of 1.0 Å for 377 Cα atoms.

HCR domains resided within the loops of the HCR_C subdomain, which are involved in protein and ganglioside dual receptor recognition (*46*). The structure of HCR/F is also similar to the isolated HCR domain of the recently solved BoNT/E structure (pdb code: 3FFZ (*47*)) with a r.m.s deviation of 0.6 Å for 324 Cα atoms (Supporting Information, Figure 5). The high degree of structural similarity between the two proteins is consistent with their highly related primary amino acid sequences (62% amino acid identity). In particular, the putative protein receptor binding pocket is highly conserved and suggests that the two serotypes may share a common protein coreceptor (Supporting Information, Figure 5).

Characterization of the HCR/F Ganglioside Binding Pocket. The interaction of BoNT serotypes A and B and TeNT with gangliosides has been extensively investigated (*23*−*27*, *48*−*52*). The cocrystal structures of HCR/T (pdb code: 1FV2) and HCR/A (pdb code: 2VU9) bound to analogues of GT_{1b} revealed a shared mechanism of ganglioside binding (*51*, *52*). In each case, the GalNAc-Gal disaccharide of GT_{1b} was found to occupy a shallow cleft on the surface of the HCR. Superposition of HCR/F with the HCR/T-GT_{1b} and HCR/A-GT_{1b} cocrystal structures showed a spatial coincidence in the carbohydrate binding site (Supporting Information, Figure 6A). Similarly, HCR/F shares a conserved H...SXWY...G motif previously identified by Binz and colleagues in HCR/A, HCR/B, and HCR/T (*26*, *27*). The corresponding motif in HCR/F is represented by His1241, Ser1248, Trp1250, Tyr1251, and Gly1263 (Supporting Information, Figure 6B). In addition, HCR/A (Glu1203) and HCR/B (Glu1190) contribute to ganglioside binding and are conserved in HCR/F (Glu 1195).

To further characterize the putative HCR/F ganglioside binding site, a series of mutated HCR/F proteins were generated (Figure 4A). Initially, amino acids homologous to the Gal-GalNAc binding site of BoNT/A were mutated and assessed for their ability to bind gangliosides. Replacement of Trp1250 with leucine caused a complete loss of binding to ganglioside

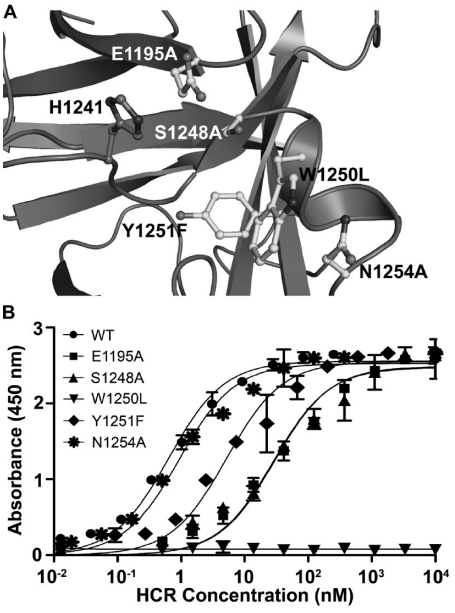

FIGURE 4: Binding of mutated HCR/F to ganglioside GT_{1b}. (A) Ribbon diagram displaying putative residues of the HCR/F ganglioside binding pocket. Residues chosen for mutation are colored in light gray. (B) The ganglioside (10 μg per well) was coated onto nonbinding microtiter plates. HCR/F or mutated HCR/F proteins at the indicated concentrations were added to the plates in Dulbecco's PBS at 4 °C for 2 h in the presence of a HRP-conjugated anti-3×FLAG antibody. Plates were washed and bound HCR detected using ultra-TMB as a substrate for HRP. The data are the average of 3 independent experiments performed in triplicate.

GT_{1b} (Figure 4B), as did replacement with alanine (data not shown). This is consistent with the requirement of the corresponding Trp residue in BoNT/A, BoNT/B, and TeNT for toxicity (*26*). Replacement of Glu1195 and Ser1248 with alanine or Tyr1251 with phenylalanine reduced binding to GT_{1b} between ~5 and 50-fold, while replacement of Asn1254 with alanine did

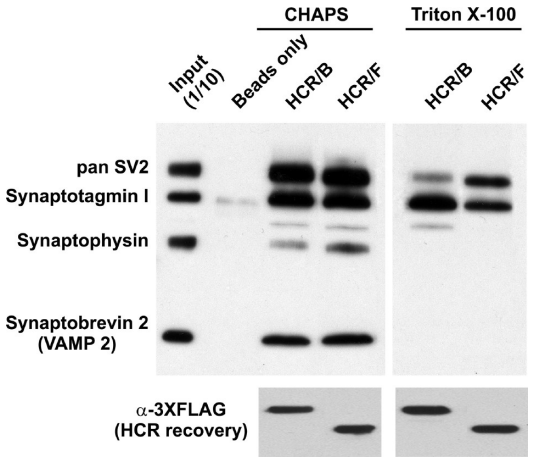

FIGURE 5: Coimmunoprecipitation of synaptic vesicle proteins with HCR/B and HCR/F. CHAPS or Triton X-100 solubilized synaptic vesicle lysates (800 μg total protein) were subjected to anti-3×FLAG precipitation with 100 nM HCR/B or HCR/F. Precipitates were separated by SDS−PAGE (12% w/v acrylamide) and analyzed by Western blotting for the presence of synaptic vesicle protein 2 (SV2), synaptotagmin I (Syt I), synaptophysin (Syp), and synaptobrevin 2 (Syb2). Data are representative of 3 independent experiments. HCR recovery was determined by running 1/20 of the eluted sample on a separate gel and detected by Western blotting using a mouse monoclonal antibody against the 3×FLAG epitope (bottom panel).

not significantly affect ganglioside binding (Figure 4B). Replacement of His1241 with alanine destabilized the protein and therefore was not studied further (data not shown). The structural integrity of the remaining mutated forms of HCR/F relative to the wild-type protein was estimated by performing limited proteolysis experiments measuring trypsin sensitivity (data not shown). These data suggest that BoNT/F associates with gangliosides through a conserved mechanism and that BoNT/F contains a single ganglioside binding site.

Protein Receptor Recognition by BoNT/F. Previous studies have identified synaptotagmins I and II as coreceptors for BoNT/B and BoNT/G (*13*, *17*), while synaptic vesicle protein 2 (SV2) mediates the entry of BoNT/A and BoNT/E into cultured hippocampal neurons (*28*, *32*, *33*). At present, there is no known protein receptor for BoNT/C, BoNT/D, or BoNT/F. To identify putative protein coreceptors for BoNT/F, entry of the toxin into cultured rat hippocampal neurons was investigated. The observation that intoxication of hippocampal neurons by BoNT/F was stimulated by active synaptic vesicle exocytosis (Figure 1B) suggested that BoNT/F may also utilize a synaptic vesicle protein as a coreceptor.

We recently reported the high affinity association of HCR/A and HCR/B with synaptic vesicle protein complexes. Solubilization of synaptic vesicle membranes in CHAPS resulted in the recovery of a large protein complex that included synaptic vesicle protein 2 (SV2), synaptotagmin I (Syt I), synaptophysin (Syp), synaptogyrin 3, synaptobrevin 2 (Syb 2), and multiple subunits of the vacuolar-type ATPase (v-ATPase) (*36*). Solubilization in octylglucoside preserved a SV2/Syt I complex, while solubilization of synaptic vesicles with Triton X-100 preserved a Syt/SV2 complex and a Syp/Syb 2 complex. These protein interactions were proposed to underlie aspects of neurotransmitter secretion, vesicle trafficking, and spatial organization within the nerve terminal. A model was proposed whereby these presynaptic protein complexes form the physiologic receptor for BoNTs (*36*).

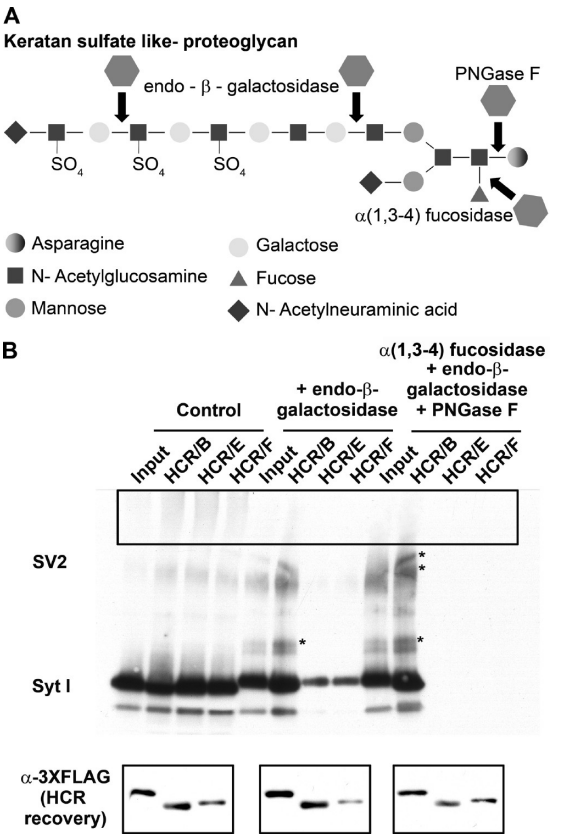

FIGURE 6: Glycosylation of SV2 is required for interaction with HCR/E and HCR/F. (A) Strategy for deglycosylation of SV2 keratan sulfate moieties by a combination of endo- and exoglycosidases. (B) Triton X-100 solubilized extracts were incubated alone, with endo-β-galactosidase, or with α(1-3,4) fucosidase, endo-β-galactosidase, and protein *N*-glycosidase F (PNGase F) for 16 h at 37 °C. Lysates were subjected to 3×FLAG immunoprecipitation with HCR/B, HCR/E, or HCR/F (final concentration of 100 nM). Precipitates were separated by SDS−PAGE (6% w/v acrylamide) and analyzed by Western blotting for the presence of synaptic vesicle protein 2 (SV2) and synaptotagmin I (Syt I). The high molecular weight forms of SV2 are boxed. New SV2 forms detected after glycosidase treatment are indicated with *. The data are representative of 3 independent experiments.

Utilizing the same strategy, interactions between synaptic vesicle proteins and HCR/F were analyzed. Precipitation of HCR/F from CHAPS detergent extracts resulted in the coprecipitation of four synaptic vesicle proteins as determined by Western blotting (SV2, synaptotagmin I, synaptophysin, and synaptobrevin 2) (Figure 5). The specificity of the association of this protein complex with HCR/F was confirmed in control reactions (beads alone, 3×FLAG-GFP) where coprecipitation of the protein complex was not detected (Figure 5 and data not shown). The analysis was repeated using an extract prepared in Triton X-100. Under these conditions, HCR/F copurified with synaptic vesicle protein 2 (SV2) and synaptotagmin I (Syt I), while other components of the neurotransmitter protein complex were not detected (Figure 5). The copurification of SV2 and synaptotagmin I under both conditions is consistent with previous studies reporting the stable association of the two proteins (*53*−*55*). Together, these observations indicate that HCR/F can bind to a similar synaptic vesicle protein complex as previously observed for HCR/A and HCR/B (*36*) and is consistent with BoNT/F intoxication of neurons being enhanced by active synaptic vesicle recycling.

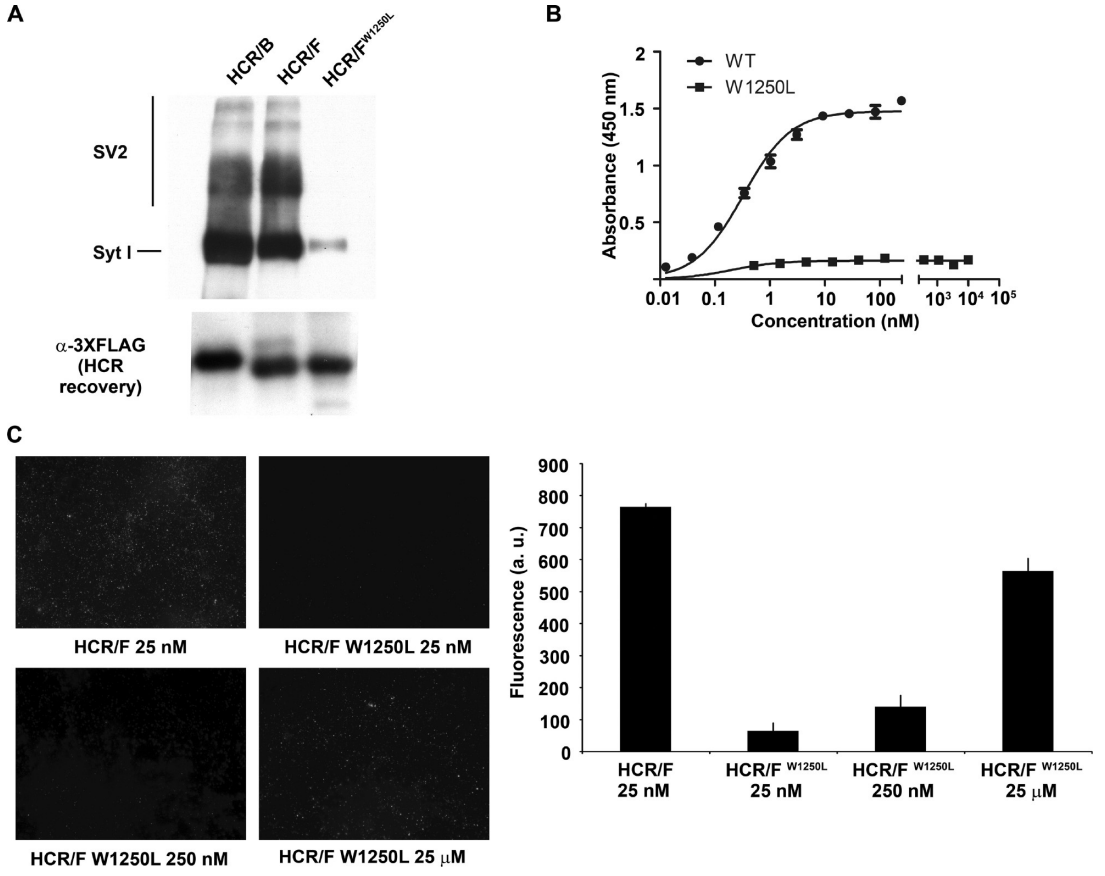

FIGURE 7: Ganglioside binding is required for SV2 interaction and neuronal binding. (A) Triton X-100 solubilized synaptic vesicle lysates were subjected to 3×FLAG immunoprecipitation with HCR/B, HCR/F, or HCR/F^{W1250L} (final concentration of 100 nM). Precipitates were separated by SDS−PAGE (6% w/v acrylamide) and analyzed by Western blotting for the presence of synaptic vesicle protein 2 (SV2) and synaptotagmin I. Membranes were subsequently reprobed using an anti-3×FLAG antibody to confirm equal loading. (B) Crude synaptic vesicles (100 ng total protein per well) were coated onto high-binding microtiter plates. HCR/F or HCR/F^{W1250L} at the indicated concentrations was added to the plates at 4 °C for 2 h in the presence of a HRP-conjugated anti-3×FLAG antibody. Plates were washed and bound HCR detected using ultra-TMB as a substrate for HRP. The data are the average of 2 independent experiments performed in quadruplicate. (C) Hippocampal neurons (DIV 10−14) were exposed to HCR/F or HCR/F^{W1250L} at the indicated concentrations for 30 min at 37 °C in fresh neurobasal medium. Cells were subsequently fixed, and bound HCRs were detected using an antibody against the 3×FLAG epitope. Binding was quantified by measuring total fluorescence of 30−40 random fields for each treatment and plotted as arbitrary fluorescence units. Nonspecific binding (no HCR domain) was subtracted from all samples. Data are representative of 2 independent experiments.

Interaction of HCR/F with Glycosylated SV2. Copurification of HCR/F with SV2/ Syt I complexes in both CHAPS and Triton X-100 extracts suggested that HCR/F may interact directly with one or both of the proteins. Indeed, BoNT/A and BoNT/B are known to directly interact with recombinant fragments of SV2 and Syt I, respectively. However, under these conditions, no interaction of HCR/F with either SV2 or Syt I was observed (*17*, *32*, *33*). A recent study by Chapman and colleagues demonstrated that entry of BoNT/E into cultured hippocampal neurons was dependent on the expression of SV2A and SV2B (*28*). The authors demonstrated that entry of BoNT/E was dependent on covalent modification of SV2, as a glycosylation deficient form of SV2 was unable to mediate BoNT/E entry. The high degree of sequence and structural homology between BoNT/E and BoNT/F suggested that the interaction of BoNT/F with SV2 or Syt I may also be dependent on covalent modification of the vesicle proteins. Moreover, the observation that HCR/F bound glycans with keratan sulfate moieties (Table 2) suggested that the interaction of HCR/F with SV2 or Syt I could be dependent on protein glycosylation (*28*).

Previous reports demonstrated that SV2 is a keratan sulfate (KS) proteoglycan (*56*, *57*). Treatment of SV2 with either protein *N*- glycosidase F (PNGase F) or endo-β-galactosidase alone resulted in modest changes in apparent molecular weight (*56*). This suggests that most of the KS chains are resistant to cleavage by endo-β-galactosidase or keratanases I and II (*56*). While the exact nature of the SV2 KS chains is unknown, modification of the core *N*-acetyllactosamine disaccharide in KS chains with fucose and sialic acid is commonly found. To determine whether glycosylation of SV2 contributes to HCR/E and HCR/F binding, conditions were established to deglycosylate native SV2 using endo-β-galactosidase. Consistent with previous reports (*56*), treatment of lysates with endo-β-galactosidase removed a small amount of carbohydrate from SV2 (Figure 6). Precipitation of HCR/E or HCR/F from lysates incubated with endo-β-galactosidase reduced the copurification of the SV2/ Syt I complex relative to control lysates as determined by Western blotting (Figure 6). Treatment of lysates with a mixture of α(1-3,4) fucosidase, endo-β-galactosidase, and PNGase F caused a loss of the high molecular weight forms of SV2 and inhibited the interaction of SV2 with HCR/E and HCR/F (Figure 6). Under the conditions used, significant change in the apparent molecular mass of Syt I was not observed upon PNGase F treatment, suggesting that the glycosidases were primarily targeting SV2. Preliminary studies of HCR/A interaction with deglycosylated SV2 have been performed, but the data at this point is

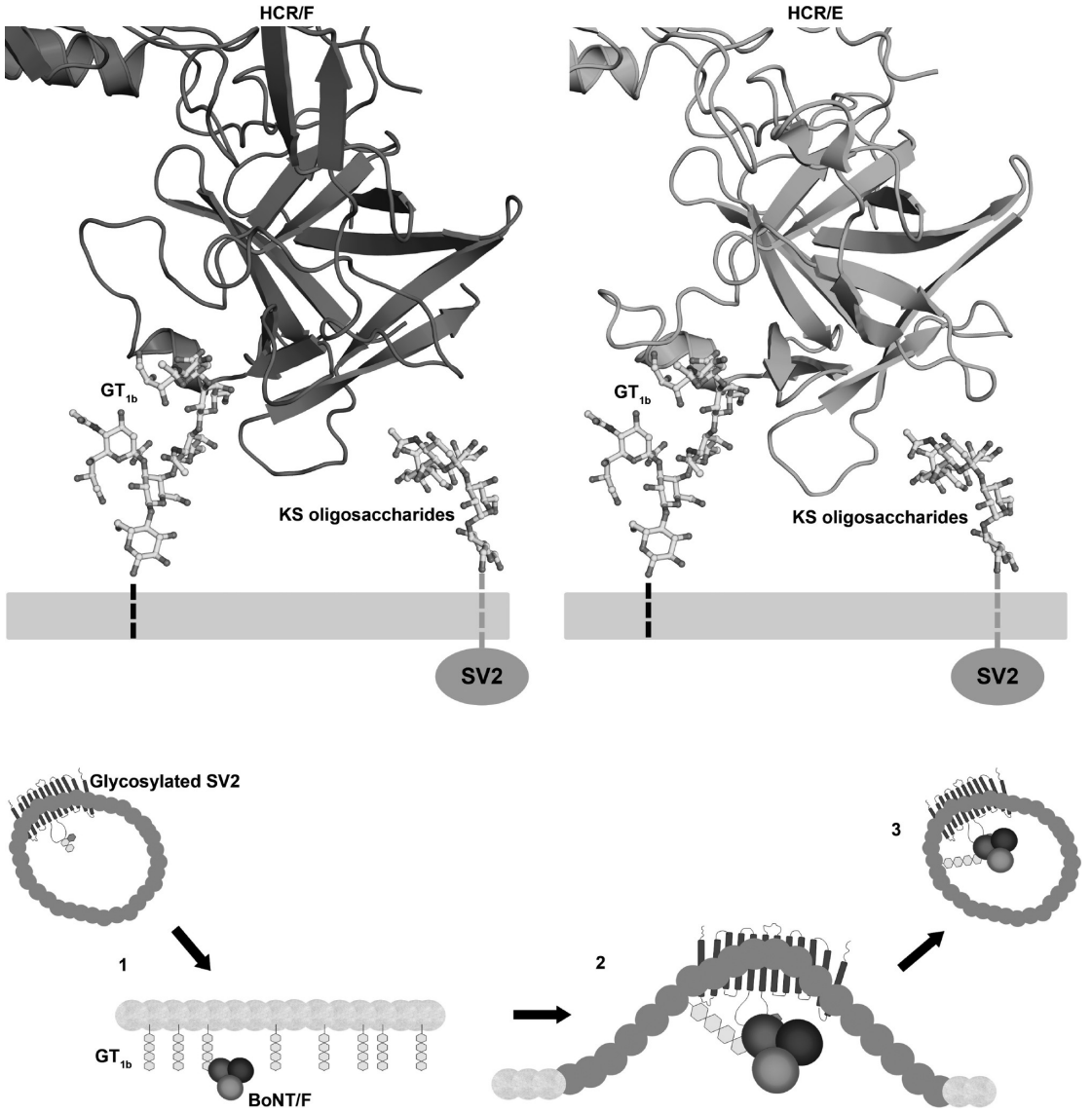

FIGURE 8: Model of HCR/F and HCR/E bound to dual carbohydrate receptors. (Upper panel) The oligosaccharide moieties of ganglioside GT_{1b} and SV2 were modeled on to the structures of HCR/F and BoNT/E (pdb code: 3FFZ). HCR/F is shown in dark gray. HCR/E is shown in light gray. The sugar molecules are displayed as ball and stick models. (Lower panel) Model for binding and entry of BoNT/F at the neuromuscular junction. BoNT/F associates with the presynaptic membrane of α-motor neurons through interactions with oligosaccharides such as ganglioside G_{T1b} (1). BoNT/F interacts with the exposed sugar moiety of SV2 following synaptic vesicle exocytosis (2). Endocytosis of synaptic vesicles drives the uptake of toxin−receptor complexes (3).

inconclusive. In contrast to HCR/E and HCR/F, treatment of lysates with the mixture of glycosidases did not inhibit the interaction of HCR/B with the SV2/ Syt I complex (Figure 6). This is consistent with previous reports demonstrating the direct interaction of the Syt I and Syt II polypeptides with BoNT/B (*13*, *16*, *17*). Together, these data suggest that both HCR/E and HCR/F bind to synaptic vesicle protein complexes primarily through the keratan sulfate moieties of native SV2. Identification of the precise oligosaccharide structure directly binding to HCR/E and HCR/F will require a detailed characterization of the SV2 KS moiety.

Ganglioside Recognition Is Required for SV2 Interaction and Neuron Binding. To further elucidate the contributions of ganglioside binding to the intoxication process, the ability of HCR/F^{W1250L} to bind to synaptic vesicle protein complexes and cultured hippocampal neurons was investigated. Under conditions where HCR/B and wild-type HCR/F bound the SV2/ Syt I complex, binding of HCR/F^{W1250L} to the SV2/ SytI complex was not observed (Figure 7A). HCR/F^{W1250L} did not bind crude synaptic vesicle membranes (Figure 7B), and binding to rat hippocampal neurons was reduced relative to HCR/F (Figure 7C), further supporting a role for ganglioside in protein coreceptor recognition.

The observation that BoNT/E and BoNT/F recognize the KS moieties of SV2 suggests that these toxins possess a second carbohydrate binding site in addition to the characterized ganglioside binding pocket. Several studies have demonstrated that tetanus HCR (HCR/T) possesses two carbohydrate binding pockets (*27*, *44*, *51*, *58*). The first characterized ganglioside binding pocket is shared by HCR/T, HCR/A, HCR/B, HCR/E, and HCR/F (Supporting Information Figure 6). The second carbohydrate binding pocket of tetanus neurotoxin is located at the distal tip of the HCR and overlaps with the synaptotagmin II binding site of BoNT/B (*16*, *44*). Arginine 1226 of HCR/T directly interacts with the disialic acid moieties of gangliosides GT_{1b} and GD_3 and is required for both carbohydrate binding and cellular toxicity (*27*, *51*). Superposition of HCR/E and HCR/F with HCR/T identified Lys1176 and Lys1199 of HCR/E and HCR/F, respectively, as the direct equivalent residues to tetanus

Arg1226 (data not shown). Thus, HCR/E and HCR/F may also coordinate an oligosaccharide at this position (Figure 8, upper panel).

The data presented here indicate that the dual receptor model can be applied to BoNT/F with the novel observation that the sugar moiety of SV2 has replaced the protein coreceptor of BoNT/B (Figure 8, upper panel). BoNT/F may interact with ganglioside concentrating the toxin on the presynaptic membrane, and subsequent to the initial capture, fusion of synaptic vesicles with the plasma membrane exposes synaptic vesicle protein luminal domains to the extracellular milieu allowing the interaction of BoNT/F with the keratan sulfate moiety of SV2 and uptake through clathrin-mediated endocytosis (Figure 8, lower panel).

ACKNOWLEDGMENT

We acknowledge the assistance of Amanda Przedpelski for HCR production. We thank the staff at the Advanced Photon Source beamline SBC 19ID for their excellent assistance in data collection.

SUPPORTING INFORMATION AVAILABLE

Structure based alignments of HCR/F with HCR/A, the HCR/F glycan binding array, and the isolated HCR domain of BoNT/E and HCR/T. This material is available free of charge via the Internet at http://pubs.acs.org.

REFERENCES

1. Arnon, S. S., Schechter, R., Inglesby, T. V., Henderson, D. A., Bartlett, J. G., Ascher, M. S., Eitzen, E., Fine, A. D., Hauer, J., Layton, M., Lillibridge, S., Osterholm, M. T., O'Toole, T., Parker, G., Perl, T. M., Russell, P. K., Swerdlow, D. L., and Tonat, K. (2001) Botulinum toxin as a biological weapon: medical and public health management. *JAMA 285*, 1059–1070.
2. Hatheway, C. L. (1995) Botulism: the present status of the disease. *Curr. Top. Microbiol. Immunol. 195*, 55–75.
3. Johnson, E. A. (1999) Clostridial toxins as therapeutic agents: benefits of nature's most toxic proteins. *Annu. Rev. Microbiol. 53*, 551–575.
4. Johnson, E. A., and Bradshaw, M. (2001) *Clostridium botulinum* and its neurotoxins: a metabolic and cellular perspective. *Toxicon 39*, 1703–1722.
5. Moller, V., and Scheibel, I. (1960) Preliminary report on the isolation of an apparently new type of CI. botulinum. *Acta Pathol. Microbiol. Scand. 48*, 80.
6. Rymkiewicz, D. (1968) Studies on *Clostridium botulinum* type F. I. Properties of selected cultures of the Langeland strain. *Med. Dosw Mikrobiol. 20*, 169–174.
7. Barash, J. R., Tang, T. W., and Arnon, S. S. (2005) First case of infant botulism caused by *Clostridium baratii* type F in California. *J. Clin. Microbiol. 43*, 4280–4282.
8. East, A. K., Richardson, P. T., Allaway, D., Collins, M. D., Roberts, T. A., and Thompson, D. E. (1992) Sequence of the gene encoding type F neurotoxin of *Clostridium botulinum*. *FEMS Microbiol. Lett. 75*, 225–230.
9. Eklund, M. W., Poysky, F. T., and Wieler, D. I. (1967) Characteristics of *Clostridium botulinum* type F isolated from the Pacific coast of the United States. *Appl. Microbiol. 15*, 1316–1323.
10. Harvey, S. M., Sturgeon, J., and Dassey, D. E. (2002) Botulism due to *Clostridium baratii* type F toxin. *J. Clin. Microbiol. 40*, 2260–2262.
11. Smith, T. J., Lou, J., Geren, I. N., Forsyth, C. M., Tsai, R., Laporte, S. L., Tepp, W. H., Bradshaw, M., Johnson, E. A., Smith, L. A., and Marks, J. D. (2005) Sequence variation within botulinum neurotoxin serotypes impacts antibody binding and neutralization. *Infect. Immun. 73*, 5450–5457.
12. Montecucco, C., Rossetto, O., and Schiavo, G. (2004) Presynaptic receptor arrays for clostridial neurotoxins. *Trends Microbiol. 12*, 442–446.
13. Dong, M., Richards, D. A., Goodnough, M. C., Tepp, W. H., Johnson, E. A., and Chapman, E. R. (2003) Synaptotagmins I and II mediate entry of botulinum neurotoxin B into cells. *J. Cell Biol. 162*, 1293–1303.
14. Chai, Q., Arndt, J. W., Dong, M., Tepp, W. H., Johnson, E. A., Chapman, E. R., and Stevens, R. C. (2006) Structural basis of cell surface receptor recognition by botulinum neurotoxin B. *Nature 444*, 1096–1100.
15. Dong, M., Tepp, W. H., Liu, H., Johnson, E. A., and Chapman, E. R. (2007) Mechanism of botulinum neurotoxin B and G entry into hippocampal neurons. *J. Cell Biol. 179*, 1511–1522.
16. Jin, R., Rummel, A., Binz, T., and Brunger, A. T. (2006) Botulinum neurotoxin B recognizes its protein receptor with high affinity and specificity. *Nature 444*, 1092–1095.
17. Rummel, A., Karnath, T., Henke, T., Bigalke, H., and Binz, T. (2004) Synaptotagmins I and II act as nerve cell receptors for botulinum neurotoxin G. *J. Biol. Chem. 279*, 30865–30870.
18. Sonnino, S., Mauri, L., Chigorno, V., and Prinetti, A. (2007) Gangliosides as components of lipid membrane domains. *Glycobiology 17*, 1R–13R.
19. Abad-Rodriguez, J., and Robotti, A. (2007) Regulation of axonal development by plasma membrane gangliosides. *J. Neurochem. 103* (Suppl 1), 47–55.
20. Bullens, R. W., O'Hanlon, G. M., Wagner, E., Molenaar, P. C., Furukawa, K., Plomp, J. J., and Willison, H. J. (2003) Roles of complex gangliosides at the neuromuscular junction. *Ann. N.Y. Acad. Sci. 998*, 401–403.
21. Yowler, B. C., Kensinger, R. D., and Schengrund, C. L. (2002) Botulinum neurotoxin A activity is dependent upon the presence of specific gangliosides in neuroblastoma cells expressing synaptotagmin I. *J. Biol. Chem. 277*, 32815–32819.
22. Kitamura, M., Takamiya, K., Aizawa, S., and Furukawa, K. (1999) Gangliosides are the binding substances in neural cells for tetanus and botulinum toxins in mice. *Biochim. Biophys. Acta 1441*, 1–3.
23. Nishiki, T., Tokuyama, Y., Kamata, Y., Nemoto, Y., Yoshida, A., Sato, K., Sekiguchi, M., Takahashi, M., and Kozaki, S. (1996) The high-affinity binding of *Clostridium botulinum* type B neurotoxin to synaptotagmin II associated with gangliosides GT1b/GD1a. *FEBS Lett. 378*, 253–257.
24. Ochanda, J. O., Syuto, B., Ohishi, I., Naiki, M., and Kubo, S. (1986) Binding of *Clostridium botulinum* neurotoxin to gangliosides. *J Biochem (Tokyo) 100*, 27–33.
25. Kitamura, M., Iwamori, M., and Nagai, Y. (1980) Interaction between *Clostridium botulinum* neurotoxin and gangliosides. *Biochim. Biophys. Acta 628*, 328–335.
26. Rummel, A., Mahrhold, S., Bigalke, H., and Binz, T. (2004) The HCC-domain of botulinum neurotoxins A and B exhibits a singular ganglioside binding site displaying serotype specific carbohydrate interaction. *Mol. Microbiol. 51*, 631–643.
27. Rummel, A., Bade, S., Alves, J., Bigalke, H., and Binz, T. (2003) Two carbohydrate binding sites in the H(CC)-domain of tetanus neurotoxin are required for toxicity. *J. Mol. Biol. 326*, 835–847.
28. Dong, M., Liu, H., Tepp, W. H., Johnson, E. A., Janz, R., and Chapman, E. R. (2008) Glycosylated SV2A and SV2B mediate the entry of botulinum neurotoxin E into neurons. *Mol. Biol. Cell 19*, 5226-5237.
29. Nishiki, T., Kamata, Y., Nemoto, Y., Omori, A., Ito, T., Takahashi, M., and Kozaki, S. (1994) Identification of protein receptor for *Clostridium botulinum* type B neurotoxin in rat brain synaptosomes. *J. Biol. Chem. 269*, 10498–10503.
30. Nishiki, T., Ogasawara, J., Kamata, Y., and Kozaki, S. (1993) Solubilization and characterization of the acceptor for *Clostridium botulinum* type B neurotoxin from rat brain synaptic membranes. *Biochim. Biophys. Acta 1158*, 333–338.
31. Nishiki, T., Tokuyama, Y., Kamata, Y., Nemoto, Y., Yoshida, A., Sekiguchi, M., Takahashi, M., and Kozaki, S. (1996) Binding of botulinum type B neurotoxin to Chinese hamster ovary cells transfected with rat synaptotagmin II cDNA. *Neurosci. Lett. 208*, 105–108.
32. Dong, M., Yeh, F., Tepp, W. H., Dean, C., Johnson, E. A., Janz, R., and Chapman, E. R. (2006) SV2 is the protein receptor for botulinum neurotoxin A. *Science 312*, 592–596.
33. Mahrhold, S., Rummel, A., Bigalke, H., Davletov, B., and Binz, T. (2006) The synaptic vesicle protein 2C mediates the uptake of botulinum neurotoxin A into phrenic nerves. *FEBS Lett. 580*, 2011–2014.
34. Baldwin, M. R., Tepp, W. H., Przedpelski, A., Pier, C. L., Bradshaw, M., Johnson, E. A., and Barbieri, J. T. (2008) Subunit vaccine against the seven serotypes of botulism. *Infect. Immun. 76*, 1314–1318.
35. Huttner, W. B., Schiebler, W., Greengard, P., and De Camilli, P. (1983) Synapsin I (protein I), a nerve terminal-specific phosphoprotein. III. Its association with synaptic vesicles studied in a highly purified synaptic vesicle preparation. *J. Cell Biol. 96*, 1374–1388.

36. Baldwin, M. R., and Barbieri, J. T. (2007) Association of botulinum neurotoxin serotypes A and B with synaptic vesicle protein complexes. *Biochemistry 46*, 3200–3210.
37. Bochner, B. S., Alvarez, R. A., Mehta, P., Bovin, N. V., Blixt, O., White, J. R., and Schnaar, R. L. (2005) Glycan array screening reveals a candidate ligand for Siglec-8. *J. Biol. Chem. 280*, 4307–4312.
38. Otwinowski, Z., and Minor, W. (1997) Processing of X-ray diffraction data collected in oscillation mode. *Methods Enzymol. 276*, 307–326.
39. Lacy, D. B., Tepp, W., Cohen, A. C., DasGupta, B. R., and Stevens, R. C. (1998) Crystal structure of botulinum neurotoxin type A and implications for toxicity. *Nat. Struct. Biol. 5*, 898–902.
40. Brunger, A. T., Adams, P. D., Clore, G. M., DeLano, W. L., Gros, P., Grosse-Kunstleve, R. W., Jiang, J. S., Kuszewski, J., Nilges, M., Pannu, N. S., Read, R. J., Rice, L. M., Simonson, T., and Warren, G. L. (1998) Crystallography & NMR system: A new software suite for macromolecular structure determination. *Acta Crystallogr., Sect. D 54*, 905–921.
41. Roussel, A., and Inisan, A. G. (1999) Turbo-Frodo, version OpenGL:1; CNRS/Universitite Marseille: Marseille, France.
42. Schiavo, G., Benfenati, F., Poulain, B., Rossetto, O., Polverino de Laureto, P., DasGupta, B. R., and Montecucco, C. (1992) Tetanus and botulinum-B neurotoxins block neurotransmitter release by proteolytic cleavage of synaptobrevin. *Nature 359*, 832–835.
43. Ogawa-Goto, K., and Abe, T. (1998) Gangliosides and glycosphingolipids of peripheral nervous system myelins: A minireview. *Neurochem. Res. 23*, 305–310.
44. Jayaraman, S., Eswaramoorthy, S., Kumaran, D., and Swaminathan, S. (2005) Common binding site for disialyllactose and tri-peptide in C-fragment of tetanus neurotoxin. *Proteins 61*, 288–295.
45. Umland, T. C., Wingert, L. M., Swaminathan, S., Furey, W. F., Schmidt, J. J., and Sax, M. (1997) Structure of the receptor binding fragment HC of tetanus neurotoxin. *Nat. Struct. Biol. 4*, 788–792.
46. Lalli, G., Herreros, J., Osborne, S. L., Montecucco, C., Rossetto, O., and Schiavo, G. (1999) Functional characterisation of tetanus and botulinum neurotoxins binding domains. *J. Cell Sci. 112* (Pt 16), 2715–2724.
47. Kumaran, D., Eswaramoorthy, S., Furey, W., Navaza, J., Sax, M., and Swaminathan, S. (2009) Domain organization in *Clostridium botulinum* neurotoxin type E is unique: Its implication in faster translocation. *J. Mol. Biol. 386*, 233–245.
48. Yowler, B. C., and Schengrund, C. L. (2004) Botulinum neurotoxin A changes conformation upon binding to ganglioside GT1b. *Biochemistry 43*, 9725–9731.
49. Kozaki, S., Kamata, Y., Watarai, S., Nishiki, T., and Mochida, S. (1998) Ganglioside GT1b as a complementary receptor component for *Clostridium botulinum* neurotoxins. *Microb. Pathog. 25*, 91–99.
50. Kitamura, M., Igimi, S., Furukawa, K., and Furukawa, K. (2005) Different response of the knockout mice lacking b-series gangliosides against botulinum and tetanus toxins. *Biochim. Biophys. Acta 1741*, 1–3.
51. Fotinou, C., Emsley, P., Black, I., Ando, H., Ishida, H., Kiso, M., Sinha, K. A., Fairweather, N. F., and Isaacs, N. W. (2001) The crystal structure of tetanus toxin Hc fragment complexed with a synthetic GT1b analogue suggests cross-linking between ganglioside receptors and the toxin. *J. Biol. Chem. 276*, 32274–32281.
52. Stenmark, P., Dupuy, J., Imamura, A., Kiso, M., and Stevens, R. C. (2008) Crystal structure of botulinum neurotoxin type A in complex with the cell surface co-receptor GT1b-insight into the toxin-neuron interaction. *PLoS Pathog. 4*, e1000129.
53. Schivell, A. E., Batchelor, R. H., and Bajjalieh, S. M. (1996) Isoform-specific, calcium-regulated interaction of the synaptic vesicle proteins SV2 and synaptotagmin. *J. Biol. Chem. 271*, 27770–27775.
54. Schivell, A. E., Mochida, S., Kensel-Hammes, P., Custer, K. L., and Bajjalieh, S. M. (2005) SV2A and SV2C contain a unique synaptotagmin-binding site. *Mol. Cell Neurosci. 29*, 56–64.
55. Lazzell, D. R., Belizaire, R., Thakur, P., Sherry, D. M., and Janz, R. (2004) SV2B regulates synaptotagmin 1 by direct interaction. *J. Biol. Chem. 279*, 52124–52131.
56. Scranton, T. W., Iwata, M., and Carlson, S. S. (1993) The SV2 protein of synaptic vesicles is a keratan sulfate proteoglycan. *J. Neurochem. 61*, 29–44.
57. Sinouris, E. A., Skandalis, S. S., Kilia, V., Theocharis, A. D., Theocharis, D. A., Ravazoula, P., Vynios, D. H., and Papageorgakopoulou, N. (2009) Keratan sulfate-containing proteoglycans in sheep brain with particular reference to phosphacan and synaptic vesicle proteoglycan isoforms. *Biomed. Chromatogr. 23*, 455–463.
58. Chen, C., Baldwin, M. R., and Barbieri, J. T. (2008) Molecular basis for tetanus toxin coreceptor interactions. *Biochemistry 47*, 7179–7186.